ResearchGate

See discussions, stats, and author profiles for this publication at: https://www.researchgate.net/publication/7995098

Magic number silicon dioxide–based clusters: Laser ablation–mass spectrometric and density functional theory studies

ARTICLE *in* JOURNAL OF COMPUTATIONAL CHEMISTRY · APRIL 2005

Impact Factor: 3.59 · DOI: 10.1002/jcc.20194 · Source: PubMed

CITATIONS
6

READS
36

10 AUTHORS, INCLUDING:

Qingyu Kong
Argonne National Laboratory
65 PUBLICATIONS **1,129** CITATIONS
SEE PROFILE

Wenning Wang
Fudan University
74 PUBLICATIONS **1,183** CITATIONS
SEE PROFILE

Can Xu
Lanzhou University
24 PUBLICATIONS **256** CITATIONS
SEE PROFILE

Kangnian Fan
Fudan University
181 PUBLICATIONS **3,811** CITATIONS
SEE PROFILE

Available from: Qingyu Kong
Retrieved on: 25 January 2016

Magic Number Silicon Dioxide-Based Clusters: Laser Ablation-Mass Spectrometric and Density Functional Theory Studies

QINGYU KONG,[1,4] LI ZHAO,[1,3] WENNING WANG,[4] CHEN WANG,[1,3] CAN XU,[1,3] WINGHAM ZHANG,[1,3] LEI LIU,[1,3] KANGNIAN FAN,[4] YUFEN LI,[2,3] JUN ZHUANG[2,3]

[1]*Department of Physics, Fudan University, Shanghai 200433, People's Republic of China*

[2]*Department of Optical Science and Engineering, Fudan University, Shanghai 200433, People's Republic of China*

[3]*State Key Joint Laboratory for Materials Modification by Laser, Ion and Electron Beams, Fudan University, Shanghai 200433, People's Republic of China*

[4]*Department of Chemistry, Fudan University, Shanghai 200433, People's Republic of China*

Received 22 September 2004; Accepted 30 November 2004

DOI 10.1002/jcc.20194

Published online in Wiley InterScience (www.interscience.wiley.com).

Abstract: The magic number silica clusters $[(SiO_2)_nO_2H_3]^-$ with $n = 4$ and 8 have been observed in the XeCl excimer laser (308 nm) ablation of various porous siliceous materials. The structural origin of the magic number clusters has been studied by the density functional theoretical calculation at the B3LYP/6-31G** level, with a genetic algorithm as a supplementary tool for global structure searching. The DFT results of the first magic number cluster are parallel to the corresponding Hartree–Fock results previously reported with only small differences in the structural parameters. Theoretical calculation predicts that the first magic number cluster $(SiO_2)_4O_2H_4$ and its anion $[(SiO_2)_4O_2H_3]^-$ will most probably take pseudotetrahedral cage-like structures. To study the structural properties of the second magic number cluster, geometries of the bare cluster $(SiO_2)_8$, the neutral complex cluster $(SiO_2)_8O_2H_4$, and the anionic cluster $[(SiO_2)_8O_2H_3]^-$ are fully optimized at the B3LYP/6-31G** level, and the corresponding vibrational frequencies are calculated. The DFT calculations predict that the ground state of the bare silica octamer $(SiO_2)_8$ has a linear chain structure, whereas the second magic number complex cluster $(SiO_2)_8O_2H_4$ and its anion $[(SiO_2)_8O_2H_3]^-$ are most probably a mixture of cubic cage-like structural isomers with an O atom inside the cage and several quasi-bicage isomers with high intercage interactions. The stabilization of these structures can also be attributed to the active participation of the group of atoms 2O and 4H (3H for the anion) in chemical bonding during cluster formation. Our theoretical calculation gives preliminary structural interpretation of the presence of the first and second magic number clusters and the absence of higher magic numbers.

© 2005 Wiley Periodicals, Inc. J Comput Chem 26: 584–598, 2005

Key words: magic number clusters; silica clusters; structure optimization; density functional theory; genetic algorithm

Introduction

Silica and related materials are of technological importance in many scientific and industrial fields. Similar to other materials, silica materials at the nanoscale may possess novel properties. An understanding of the structures, stability, and properties of silica nanoparticles and clusters could aid the exploration of their new applications. In our recent laser ablation experiments of porous siliceous materials, we developed a method for the efficient generation of SiO_2-based clusters. With this novel method we have performed a systematic investigation of silica cluster generation from a variety of porous siliceous materials.[1–4] The phenomenon that has attracted our particular interest is the first observation of magic number silica-containing clusters $[(SiO_2)_nO_2H_3]^-$ (n = 4,8), which has been reported in our previous artricle.[5] In the XeCl excimer laser ablation mass spectra, several silica-containing cluster sequences are produced, but only the $[(SiO_2)_nO_2H_3]^-$ sequence displays magic number cluster behavior. The appearance of magic number clusters is usually an indication of the special stability of the clusters with those particular compositions. Therefore, the discovery of magic number clusters may often lead to new cluster

Correspondence to: J. Zhuang; e-mail: Zhuang1022@yahoo.com

Contract/grant sponsor: The National Natural Science Foundation of China; contract/grant numbers: 10004002 and 29890216

© 2005 Wiley Periodicals, Inc.

materials, which, if made in bulk quantity, might exhibit novel properties and have new applications, such as for example the buckminsterfullerene C_{60}. To understand the structural origin of magic number clusters is thus an interesting and important step toward the exploitation of new silica cluster materials.

However, the structure investigation of clusters is a challenge to scientists, both experimentally and theoretically. Although the experimental determination of cluster structures has progressed in the last 2 decades, its feasibility and applicability are still quite limited. For most of the clusters it is difficult to obtain unambiguous structural information from experiments, so theory has a particularly important role to play. For the magic number complex clusters studied in this article no experimental information about their structures is currently available. Therefore, we have to resort to theoretical modeling.

In our previous artilce about the magic number silica clusters, the generation, formation mechanism, and the structure study of the $n = 4$ magic number cluster at the Hartree–Fock level were reported and discussed.[5] In the present article, calculation results using the density functional theory will be reported with emphasis on the $n = 8$ silica clusters to account for the appearance of the second magic number cluster in the mass spectra. In our calculation, genetic algorithm (GA) was used as supplementary means to help searching for the isomer structures.

Experimental and Computational Methods

Experimental

The experimental apparatus and techniques have been described in our previous articles.[1–5] A 308 nm XeCl excimer laser was used for the generation of silica clusters, and time-of-flight (TOF) mass spectrometry was employed for studying the abundance distribution of the clusters. The mass spectrometric measurement was concentrated in the negative ion channel, because for the silica clusters rich information has only been observed in the negative ion mass spectra. A reflectron TOF mass spectrometer of mass resolution $M/\Delta M \sim 1000$ was used to determine the chemical composition of the magic number cluster sequence.

A variety of porous siliceous materials have been investigated, but only some surface SiOH-rich samples can effectively generate the magic cluster sequence and so were studied in detail. Rhodamine dye-doped silica aerogel, carbon-doped silica aerogel, azo dye-doped xerogel, and some colored silica gels are samples suitable for this purpose. The effect of doping on the generation of clusters has been discussed in our previous article.[1] The preparation of the Rhodamine 6G-doped silica aerogel has been described therein.[1] The azo dye-doped xerogel was prepared by the usual sol-gel technique with an azo dye as the dopant, and the blue silica gel sample was the commercial desiccant.

For comparison, mass spectrum of a surface SiOH-deficient sample—the hydrothermal-treated silicalite-1–was also presented.

Theoretical

The search for the ground-state configuration of clusters belongs to a class named NP-hard optimization problems. The choice of initial candidate structures of the cluster isomers is of paramount importance to the success of the optimization. Therefore, an efficient method of obtaining these starting structures for the optimization is highly desirable. Genetic algorithm is one of such methods for this purpose. In our case of silica-containing clusters, first we build the initial structures on the basis of known silica structural principles and the related isomer structures reported previously. In addition, we use genetic algorithm to aid our searching of the configuration spaces relevant to the silica clusters studied in the present article.

In our previous article[5] the structures of the bare silica cluster $(SiO_2)_4$ and the first magic number cluster $[(SiO_2)_4O_2H_3]^-$ and its precursor $(SiO_2)_4O_2H_4$ optimized with *ab initio* molecular orbital techniques at the Hartree–Fock level with the 6-31G** basis set were reported. In the present article, we perform the density functional theoretical calculations on the first and second magic number silica clusters in detail using the Gaussian 98 program package.[6] The Becke three-parameter hybrid functional with the Lee–Yang–Parr correlation corrections (B3LYP) was used.[7,8] This hybrid functional can provide reliable predictions of the state energies, structures, and vibrational frequencies of small organic molecules and metal containing compounds,[9–11] and thus has been widely used in recent years. The 6-31G** basis set was used for the Si, O, and H atoms.[12,13] In our calculations, geometries were fully optimized and the vibrational frequencies were calculated with analytical second derivatives. Besides the anionic magic number clusters $[(SiO_2)_4O_2H_3]^-$ and $[(SiO_2)_8O_2H_3]^-$, the results of the bare silica clusters and the neutral complex precursors were also given.

Genetic algorithm is a stochastic global minimization technique inspired by concepts from Darwinian natural evolution.[14] Populations of candidate solutions compete with each other for survival. The ultimate surviving individual is the best solution of the optimization problem, and in our case, is the lowest energy structure of the cluster. In this article genetic algorithm was employed for sampling the structural configuration spaces, and some special interesting low-energy structures or structure skeletons have been generated and can be used for the building of complex magic number clusters. According to the composition of the magic number cluster sequence, the configuration space corresponding to the bare silica clusters composed of $nSiO_2$ as well as the configuration space $nSiO_2+2O$ corresponding to the complex cluster skeleton were searched in our recent studies. The bare and complex clusters are finally optimized by the density functional theory, from which reliable minimal energy values of the cluster isomers can be obtained. A comparison of the DFT energy values of the isomers can thus lead to reliable energetic ordering of the isomers. By taking advantage of the combination of empirical genetic algorithm search and DFT optimization, the investigation of the global minimal energy structures of the magic number clusters has been achieved. We think that the lowest energy structures presented in this article might be the most probable ground-state structures. Of course, we cannot guarantee that we have really reached the global minima representing the ground states of the magic number clusters because of the structure complexity of the clusters, especially for the second magic number cluster.

Because in this article the genetic algorithm was only used as a supplementary tool, and it has been described several times in our other works,[15–17] we shall not discuss its performance in detail here. Briefly, first we create a population of candidate structures at random for the cluster, in which the candidates are relaxed to their

nearest local energy minima. The species or candidate in the population is characterized by the fitness, which in our case is related to its potential energy. Then, from these candidates, two of them are selected as "parents" for "mating" with a selection probability depending on their fitness. In the mating process, random planes are used to cut the "father" and "mother" structures into half structures, respectively. We then assemble the half structures to form the "child" structure by joining one part of the father to one part of the mother. After that, the child is relaxed to its local minimum. If its energy is lower than that of the highest energy candidate in the population and its structure is not similar to any other candidate structure, then the child is selected for inclusion in the population. At the same time, the candidate with the highest energy is eliminated for conserving the number of candidates in the population. Thus, the new or next generation of the population is formed. The process from the selection of parents to the formation of the next generation is considered as one evolution step. By repeating the process, the population is evolved. In our calculation, the silica cluster is modeled by the TTAM potential.[18] Because the TTAM potential was developed for the condensed phase siliceous materials, the use of such potential to describe the structure of silica cluster is an approximation, which means that the lowest energy structure we obtained by GA is probably incorrect. For example, the lowest energy structure of the tetramer $(SiO_2)_4$ given by our GA with TTAM potential is a 3D cage structure (see Fig. 3a), while it is known that the lowest energy isomer of $(SiO_2)_4$ has a linear chain structure. Fortunately, however, the aim of the GA searching with the TTAM potential in this work is simply to supply a variety of skeletons to be used for the construction of the initial complex silica-containing structures to be used for further DFT optimization. Therefore, the main task of the GA searching in the present work is to give a group of lower energy structures, and the final most stable structure is determined by DFT optimization. For this purpose, in our genetic algorithm, the evolution process is not stopped until the structures of half of the species with lower energies in the population remain unchanged in succeeding evolution steps. Based on the lower energy structures of the bare silica clusters generated by GA, the structures of the complex silica clusters are then constructed. As the molecular compositions of the magic number clusters contain two extra O atoms in addition to $(SiO_2)_n$, to make the construction of the structure of the magic number cluster easier, we also did the GA searching for the configuration space $nSiO_2+2O$. The advantage of the $nSiO_2+2O$ searching over the $nSiO_2$ searching will be clear through the following description in the present article.

Results and Discussion

Mass Spectrometric Results

Figure 1 depicts the typical anionic mass spectra of porous siliceous materials obtained under XeCl excimer laser ablation. The general features are: in the negative ion channel several $(SiO_2)_n$-containing cluster sequences $(SiO_2)_n^-$ and $[(SiO_2)_nX]^-$ with X=H,O,OH,O_2H_3, . . .have been observed, where Xs are dependent upon the properties of the samples in general and the surface states of the samples in particular. Here we focus our attention on the particular cluster sequence $[(SiO_2)_nO_2H_3]^-$, which shows evidence of magic numbers $n = 4,8$. For most of the samples we studied, $[(SiO_2)_n]^-$ (and/or $[(SiO_2)_nH]^-$) and $[(SiO_2)_nO]^-$ (and/or$[(SiO_2)_nOH]^-$) are the two most prominent sequences. Although their abundance distributions vary with samples and experimental conditions, the distributions are always normal, that is, with no noticeable discontinuities in the mass spectra. In contrast, the sequence $[(SiO_2)_nO_2H_3]^-$ always displays anomalous mass abundance patterns, with sharp discontinuities at $n = 4$, 8, as shown in the typical mass spectra in Figure 1a, b, and c. In other words, 4 and 8 are the magic numbers of this cluster sequence. The intensity of this sequence varies greatly with samples, and is relatively abundant for SiOH-rich samples, such as doped silica aerogel and some porous amorphous silica samples. But for surface SiOH-deficient samples, such as hydrothermal-treated silicalite-1, this magic number sequence practically disappears with the simultaneous shortening of the two main cluster sequences, as shown in Figure 1d. Although the intensity of the magic cluster sequence varies with samples, the compositions of the magic cluster sequence remain unchanged, that is, $[(SiO_2)_nO_2H_3]^-$, in which X has been ascertained to be O_2H_3 through mass spectrometric measurement on our reflectron mass spectrometer.[5] A comparison of Figures 1a to d indicates that not only the intensity of the magic number cluster sequence varies with samples, but also the abundance distribution in the mass spectrum shows some dependence on sample properties and/or experimental conditions. We found that, in general, $n = 4$ and 8 are magic numbers, but the intensity of the $n = 5$ cluster, $[(SiO_2)_5O_2H_3]^-$, also shows some abnormality. Figures 1a and b illustrate the usual magic behavior, but in Figure 1c of azo dye-doped silica xerogel, in addition to the strong magic number clusters with $n = 4$ and 8, the cluster $n = 5$ is also abundant with intensity similar to the cluster $n = 4$. Such intensity distribution also appears in some other samples, such as the carbon-doped silica aerogel sample. We will discuss this phenomenon in a later section.

For all the siliceous samples investigated, no silica clusters have been observed in the positive ion channel. Therefore, only the structures of the anionic magic number clusters and their neutral precursors are calculated and discussed.

Theoretical Modeling

As the bare silica cluster sequence $[(SiO_2)_n]^-$ shows normal abundance distribution and only the sequence $[(SiO_2)_nO_2H_3]^-$ displays magic behavior on the mass spectra, it is reasonable to consider that the group of atoms composed of 2O and 3H (not necessarily as a single radical or ligand) must be actively involved in chemical bonding to stabilize the magic number clusters. We attempt to find out the structural origin of the magic behavior through theoretical modeling in the following. Our genetic algorithm searching provides a rich variety of candidate structures for the construction of the first and second magic number clusters, especially the $nSiO_2+2O$ searching. Therefore, our calculation of the first magic number cluster with the density functional theory is more extended than the Hartree–Fock calculation reported in the previous article. For the second magic number cluster, the structures of the neutral and anionic complex magic number clusters $(SiO_2)_8O_2H_4$ and $[(SiO_2)_8O_2H_3]^-$ are formed by adding the group of O and H atoms

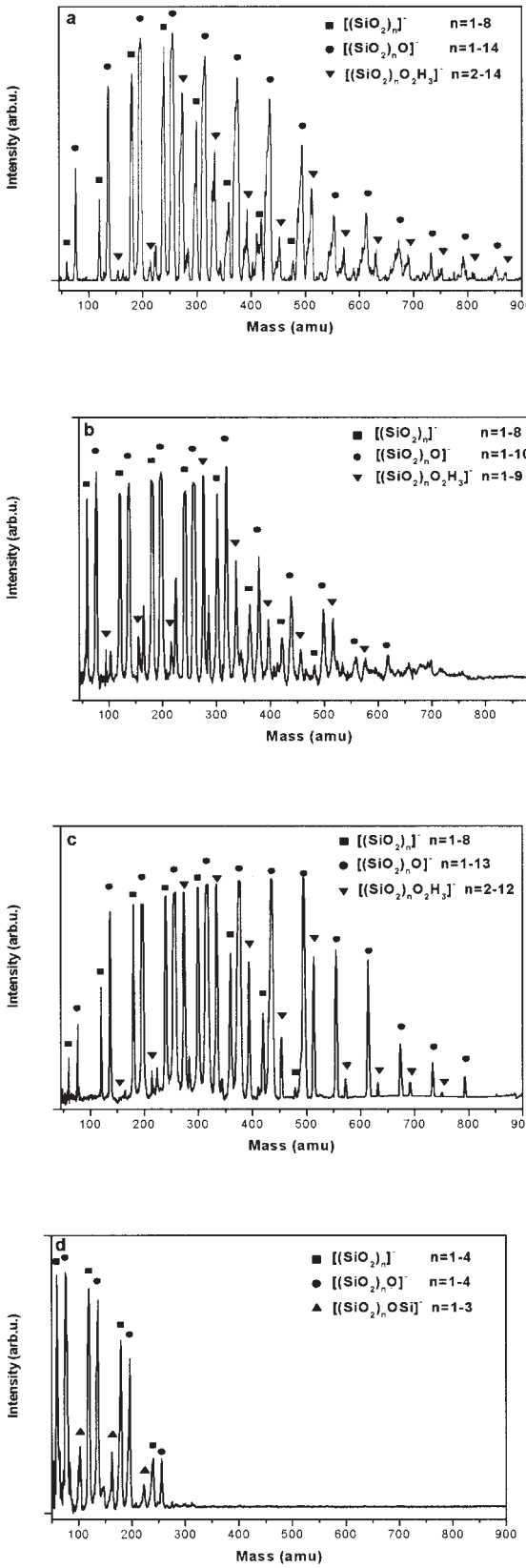

to the bare silica cluster structures or adding only H atoms to the Si—O skeleton structures obtained by GA and then optimized by DFT. Also, complex cubic and linear structures of $(SiO_2)_8O_2H_4$ formed by adding the group of O and H atoms to simple cubic and linear structures of bare $(SiO_2)_8$, and a bicage isomer of $(SiO_2)_8O_2H_4$ formed by doubling the cage structure of the first magic number cluster, are also optimized, and their energies are compared with those of other isomers.

The calculation in this article consists of two parts. The first part contains the calculation on the $n = 4$ magic number cluster with the density functional theory. More structural isomers were discussed. An interpretation of the anomalous behavior of the $n = 5$ cluster was attempted. The second part reports the detailed DFT calculation on the $n = 8$ magic number cluster and the related species, which have not been touched in our previous article. Here, the important role played by genetic algorithm is clearly illustrated.

DFT Calculation on n = *4 Magic Nnumber Silica Cluster:* $(SiO_2)_4O_2H_4$

Genetic algorithm searching of the configuration spaces $4SiO_2$ and $4SiO_2+2O$ gives the lowest energy structures shown in Figure 2a and b, respectively, from which the magic number cluster can be derived. The advantage of $nSiO_2+2O$ searching is obvious, because the Si—O skeleton of $4SiO_2+2O$ shows the positions of all the terminal O atoms and so the magic number cluster can be formed simply by adding H atoms to the O terminals, which is simpler than adding O and H atoms to the bare $(SiO_2)_4$.

We performed structural optimization of the lower energy isomers of $(SiO_2)_4$, neutral $(SiO_2)_4O_2H_4$, and anionic $[(SiO_2)_4O_2H_3]^-$ using the density functional theory at the B3LYP/6-31G** (6-31+G** for the anions) level. All the DFT structures are similar to the corresponding HF ones with only small differences in the structural parameters. For example, the bond lengths of the magic number cluster $[(SiO_2)_4O_2H_3]^-$ calculated at B3LYP/6-31+G** level are bigger than those at HF/6-31+G** level by less than 2%. Here, only the optimized energy values of the structural isomers of $(SiO_2)_4O_2H_4$ are listed in Table 1 and the corresponding structures depicted in Figure 3. The stability orders of the isomers are the same for HF and DFT. Similar parallelism exists between the HF and DFT results for the bare $(SiO_2)_4$ and anionic $[(SiO_2)_4O_2H_3]^-$ (not presented here). Besides the structures listed in our previous article, more structures with lower energy of $(SiO_2)_4O_2H_4$ can be formed from candidate structures obtained by $4SiO_2+2O$ searching, of which some are also included in Table 1 and Figure 3. The formation of Si_2O_2 rhombus in the ring structures lowers the energy of the isomers, such as in the

Figure 1. Typical mass spectra of $[(SiO_2)_nX]^-$ cluster anions obtained by the XeCl excimer laser ablation of (a) Rhodamine 6G-doped silica aerogel, (b) blue silica gel, (c) azo dye-doped silica xerogel, and (d) surface SiOH-deficient sample—hydrothermal-treated silicalite-1. (■) $[(SiO_2)_n]^-/[(SiO_2)_nH]^-$, (●) $[(SiO_2)_nO]^-/[(SiO_2)_nOH]^-$, and (▼) $[(SiO_2)_nO_2H_3]^-$.

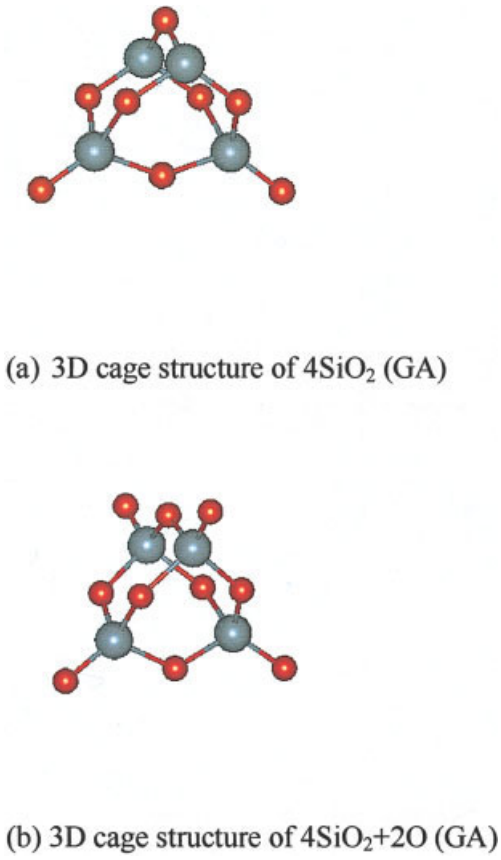

Figure 2. Lowest energy structures generated by the genetic algorithm searching of (a) the $4SiO_2$ and (b) the $4SiO_2$+2O configuration spaces.

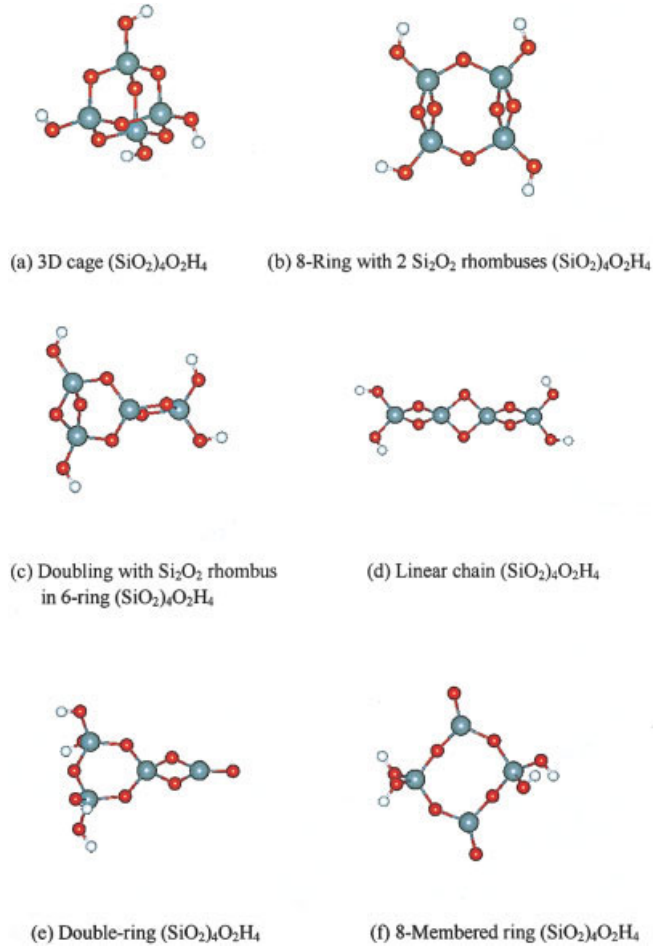

Figure 3. B3LYP/6-31G** optimized structures of the ground state and some higher energy isomers of the neutral $(SiO_2)_4O_2H_4$ complex clusters: (a) 3D cage, (b) eight-ring with two Si_2O_2 rhombus, (c) double-ring with Si_2O_2 rhombus in six-ring, (d) linear chain, (e) double-ring, and (f) eight-ring, in the order of descending stability.

cases of the eight-ring and the double-ring isomers. However, all these structural isomers are higher in energy than the cage isomer. Although these new structural isomers would form anionic clusters with energies lower than those of the eight-ring and double-ring isomers, the 3D cage anionic cluster is still the lowest energy isomer. Taking all isomers obtained in our calculation into consideration, the much lower energies of the cage isomers of $(SiO_2)_4O_2H_4$ and $[(SiO_2)_4O_2H_3]^-$ suggest that the magic number cluster $n = 4$ will most probably take the cage-like structures. The bonding characteristics in the isomers of the neutral and anionic magic number clusters have been analyzed in our previous article[5] and will not be repeated here.

In our energy calculation of the complex cluster isomers, it was found that the energy of the complex silica cluster is mainly determined by the Si—O structure skeleton, and the directions of

Table 1. Optimized Energies of Structural Isomers of Neutral Complex Silica Cluster $(SiO_2)_4O_2H_4$ Calculated at HF and B3LYP Levels with the 6-31G** Basis Set.

Structure	E(HF/6-31G**) (Hartree)	E(B3LYP/6-31G**) (Hartree)
3D cage-like	−1907.48575	−1913.38884
Eight-Ring with 2 Si_2O_2 rhombus	−1907.42375	−1913.33263
Double-ring with Si_2O_2 rhombus in six-ring	−1907.39794	−1913.30849
Linear chain	−1907.37887	−1913.29328
Double-ring	−1907.35216	−1913.27097
Eight-ring	−1907.29135	−1913.21428

the terminal OHs have only a slight effect. For example, the energy difference between the neutral linear chain complex isomers $(SiO_2)_4O_2H_4$ with different end OH directions is much smaller than the difference between isomers with different structure skeletons. Therefore, in the following discussion we shall not differentiate the structural isomers with different terminal OH directions.

In short, we believe that the first magic number cluster $n = 4$ will most probably take the cage-like structure: the ground state of the neutral $(SiO_2)_4O_2H_4$ cluster has a pseudotetrahedral structure with S_4 symmetry and that of the anionic magic number cluster $[(SiO_2)_4O_2H_3]^-$ is a distorted pseudotetrahedral structure with C_3 symmetry. The peculiar 3D structure of the bare cluster $(SiO_2)_4$ provides adequate sites for ideal chemical bonding. Such a situation does not exist for bare silica clusters with $n = 3$ or 5. Therefore, it is clear that the magic number $n = 4$ originates from the special cage-like structure of the complex $n = 4$ cluster in which all the bonding requirements of the constituent atoms are nearly perfectly satisfied. No imaginary frequencies were found in the frequency calculation of $[(SiO_2)_4O_2H_3]^-$ at the B3LYP/6-31+G** level, indicating that the cage-like structure is the energy minimum on the potential energy surface of the magic number cluster.

We have also optimized the structure of the magic number anionic cluster $[(SiO_2)_4O_2H_3]^-$ with a larger basis set 6-311++G** and found that the structural parameters are practically the same as with 6-31+G**, implying that for such cluster systems B3LYP/6-31G** for the neutral and B3LYP/6-31+G** for the negative ions are the appropriate levels for structural optimization. Therefore, these same levels were used for the calculation of the second magic number cluster.

From an inspection of the mass spectra in which the magic cluster sequence plays a significant role, we found that although the $n = 4$ cluster $[(SiO_2)_4O_2H_3]^-$ is usually the strongest magic number cluster, but in some spectra the $n = 5$ cluster is also quite intense, as mentioned above. As the formation of the complex clusters involves a complicated reaction path, the intensity distribution of the cluster species depends not only on the relative stabilities of the species, but also on the sample properties and experimental conditions. As we know from the previous works and our calculation to be mentioned below, the bare silica clusters $(SiO_2)_n$ with $n \leq 8$ have linear chain structures as their most stable isomers. Our laser ablation study indicates that the bare silica cluster sequence $[(SiO_2)_n]^-$ (and/or $[(SiO_2)_nH]^-$) and the strongest sequence $[(SiO_2)_nO]^-$ (and/or$[(SiO_2)_nOH]^-$) have normal abundance distribution in the mass spectra of siliceous materials. This phenomenon implies that for these two cluster sequences the clusters do not change their structure type as they grow in size. For example, the bare silica cluster sequence $[(SiO_2)_n]^-$ (at least for $n \leq 8$) all take the linear chain structures. In our previous article on magic number silica clusters we have made a preliminary discussion on the formation mechanism of the magic number cluster sequence, which is closely related to the two normal sequences.[5] Moreover, we have demonstrated that the appearance of the magic number 4 originates from the formation of the cage-like structure of $[(SiO_2)_4O_2H_3]^-$ with peculiar stability. Therefore, from the thermodynamic point of view, $n = 4$ should be the magic number. But the cage-like structure is formed through the transformation of the chain structure to the cage structure during complex cluster formation, which might be kinetically slower than the transformation between chain structures like in the $n = 5$ case. That is to say, on the one hand, thermodynamic consideration favors the $n = 4$ complex cluster, while on the other hand, kinetic consideration probably prefers the $n = 5$ complex cluster. There might exist a competition between the formation of the $n = 4$ and $n = 5$ species in the magic cluster sequence, which leads to the change of the abundance distribution mentioned above. As such competition is related to the sample properties and experimental conditions, this might explain what we observed in our experiments, that is, the relative intensity of the $n = 5$ cluster with respect to that of the $n = 4$ cluster in the magic number cluster sequence changes from spectrum to spectrum.

DFT Calculation on n = 8 *Magic Number Silica Cluster:* $(SiO_2)_8O_2H_4$ *and* $[(SiO_2)_8O_2H_3]^-$

As the second magic number cluster $[(SiO_2)_8O_2H_3]^-$ contains twice the number of SiO_2 units compared to the first magic number cluster $[(SiO_2)_4O_2H_3]^-$, we think that their structures might be closely related. At first glance, we might imagine a probable structure for the neutral $n = 8$ cluster $(SiO_2)_8O_2H_4$ by doubling the cage structure of $(SiO_2)_4O_2H_4$ to form a bicage consisting of two pseudotetrahedral $n = 4$ structural units connected through two oxygen bridges. Another possible structure of $(SiO_2)_8O_2H_4$ might be of the cubic type because it is well known that cubic structure may exist in siliceous materials. Also, we have used genetic algorithm to search the configuration spaces $8SiO_2$ and $8SiO_2+2O$, and the results are exciting. A great deal of new candidate structures are obtained. Here, we shall only take some of the lower energy candidates in GA search into consideration, of which the lowest energy skeleton is cubic and the next two skeletons are bicage-like, called quasi-bicage in the following. Finally, the linear chain structure is included for comparison. In general, the bare $(SiO_2)_8$ or Si—O skeleton of $8(SiO_2)+O_2$ are constructed first and then the complex clusters $(SiO_2)_8O_2H_4$ are formed by adding the group of atoms 2O and 4H to the former or only 4H to the latter. All these model structures are then optimized with the DFT approach.

The Cubic Isomers of $(SiO_2)_8O_2H_4$

The structure of the simple cubic $(SiO_2)_8$ was constructed from Si—O tetrahedrons and then optimized at the B3LYP/6-31G** level. The structure depicted in Figure 4d shows that the optimized structure is a distorted cube. This is reasonable, because only four Si atoms on alternate cube corners are connected to terminal O atoms, causing the distortion of the cube. For clarity we also show the structure in projective view that illustrates the distortion more clearly.

Similar to the case of the first magic number cluster, the genetic algorithm searching of the $8SiO_2$ and $8SiO_2+2O$ configuration spaces gives interesting results. Figure 5a and b show the lowest energy structures given by searching the two spaces. Figure 5a shows that the lowest energy isomer also has a cubic structure but it is different from the one we have just built. In the structure generated by GA, one of the terminal O atoms points toward the

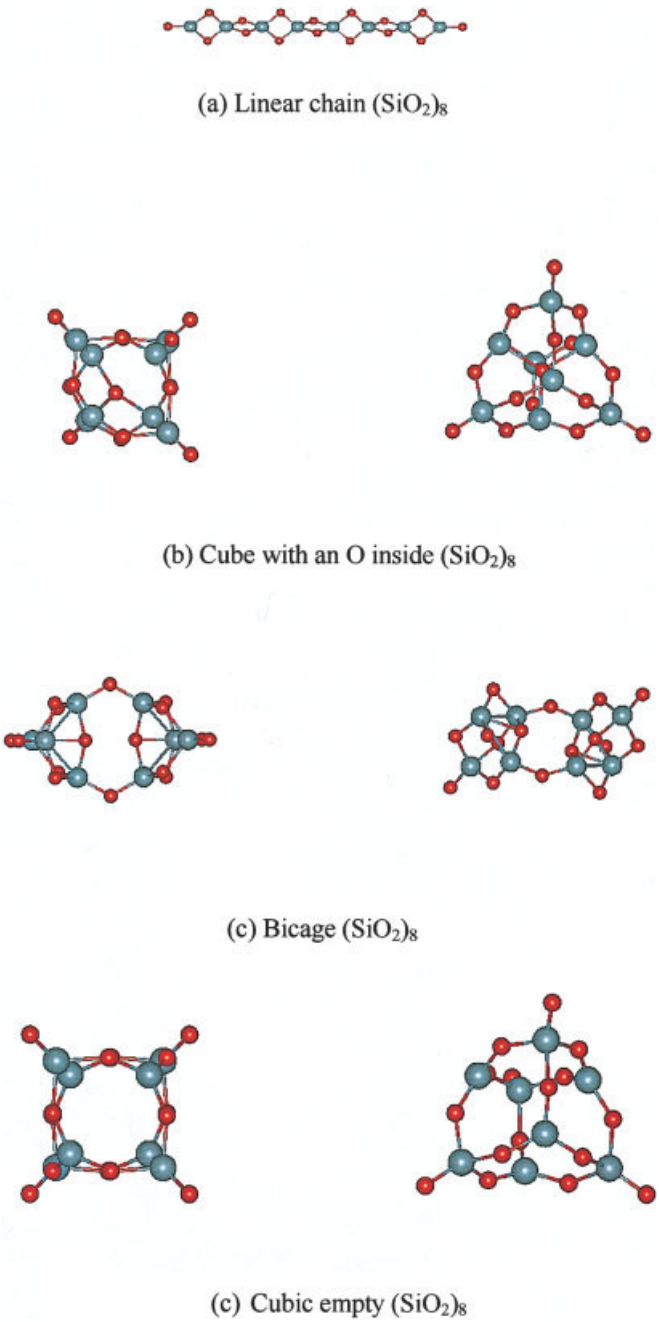

Figure 4. B3LYP/6-31G** optimized structures of the ground state and the next higher energy isomers of the bare $(SiO_2)_8$ clusters in the order of descending stability: (a) linear chain, (b) two views of cubic structure with an O inside the cage, (c) two views of bicage structure, and (d) two views of cubic empty structure. [Color figure can be viewed in the online issue, which is available at www.interscience.wiley.com.]

center of the cube. The structure after DFT optimization is presented in Figure 4b. The energy values listed in Table 2 show that the structure with inside O atom is more stable than the empty

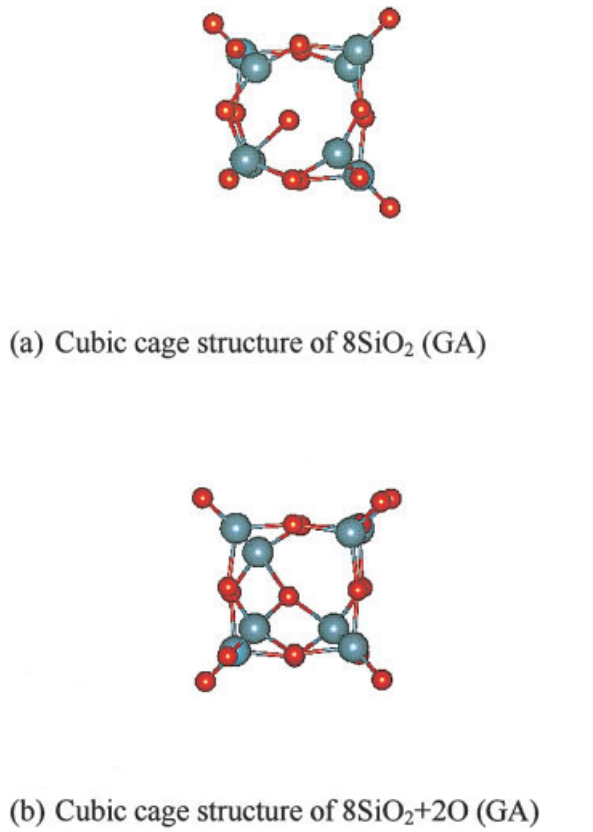

Figure 5. Lowest energy structures generated by the genetic algorithm searching of (a) the $8SiO_2$ and (b) the $8SiO_2$+2O configuration spaces. [Color figure can be viewed in the online issue, which is available at www.interscience.wiley.com.]

cubic one. The reason may be that the interaction between the negatively charged inside O atom and the positively charged silicon cage stabilizes the cluster. Our DFT calculation shows that the inside O atom carries more negative charge than other O atoms in the cluster. Here the merit of genetic algorithm is obvious, because without taking advantage of GA approach, it is hardly possible for us to imagine the unusual cubic silica structure with an inside oxygen atom.

The neutral complex cubic structure $(SiO_2)_8O_2H_4$ is formed by adding the group of atoms 2O and 4H to the proper positions of the

Table 2. Optimized Energies of Structural Isomers of Bare Silica Clusters $(SiO_2)_8$ Calculated at the B3LYP/6-31G** Level.

Structure	Symmetry	E (Hartree)	ΔE (Hartree)[a]
Linear chain	C_{2h}	−3520.59864	0
Cubic with an O inside	C_1	−3520.58874	0.00990
Bicage	C_2	−3520.51098	0.08766
Cubic empty cage	D_2	−3520.46840	0.13024

[a]The Δ column in the table show the energy differences of the isomers with respect to the lowest energy isomers (same for Tables 3 and 4).

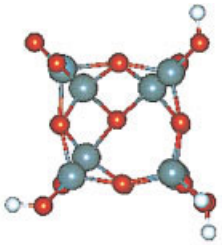

(a) Cubic structure $(SiO_2)_8O_2H_4$ with inside O

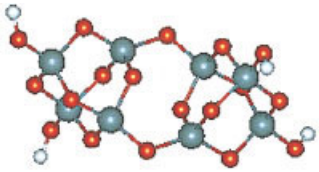

(d) Bicage structure $(SiO_2)_8O_2H_4$

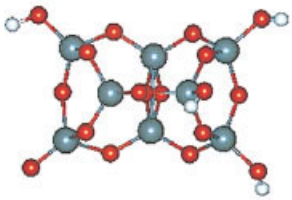

(b) Quasi-bicage structure $(SiO_2)_8O_2H_4$ (Type I)

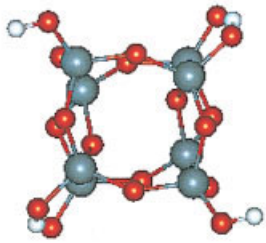

(e) Cubic empty cage structure $(SiO_2)_8O_2H_4$

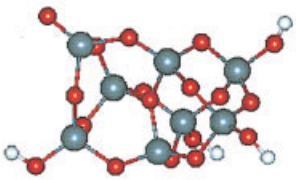

(c) Quasi-bicage structure $(SiO_2)_8O_2H_4$ (Type II)

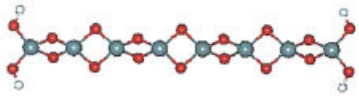

(f) Linear chain structure $(SiO_2)_8O_2H_4$

Figure 6. B3LYP/6-31G** optimized structures of the ground state and the next higher energy isomers of the neutral $(SiO_2)_8O_2H_4$ complex clusters in the order of descending stability: (a) cubic structure with an O inside the cage, (b) quasi-bicage structure (Type I), (c) quasi-bicage structure (Type II), (d) bicage structure, (e) cubic empty structure, and (f) linear chain structure. [Color figure can be viewed in the online issue, which is available at www.interscience.wiley.com.]

bare cubic structures. From the simple cubic structure in Figure 4d, the corresponding structure of the complex cluster after DFT optimization is shown in Figure 6e in the projective view. It is evident that the addition of the group of atoms 2O and 4H causes the high distortion of the complex cluster. Complex cubic structure can similarly be formed from the silica octamer with an O atom

Table 3. Optimized Energies of Structural Isomers of Neutral Complex Silica Cluster $(SiO_2)_8O_2H_4$ Calculated at the B3LYP/6-31G** Level.

Structure	ZPE (kcal/mol)	E (Hartree)	ZPE + E (Hartree)	Δ(ZPE + E) (Hartree)[a]
Cubic with an O inside	84.91243	−3673.84303	−3673.70772	0
Quasi-bicage (Type I)	84.89325	−3673.83750	−3673.70223	0.00549
Quasi-bicage (Type II)	84.99071	−3673.83314	−3673.69770	0.01002
Bicage	85.26852	−3673.77618	−3673.64029	0.06743
Cubic empty cage	84.63396	−3673.73368	−3673.59888	0.10884
Linear chain	83.83259	−3673.68149	−3673.54790	0.15982

inside. Here, once again, the advantage of $nSiO_2+2O$ searching is obvious, as illustrated for the lowest energy skeleton in Figure 5b, in which the terminal O atoms where H atoms can be attached are clearly demonstrated. The neutral magic number cluster precursor can be formed from this Si—O skeleton simply by adding 4H atoms to the proper O terminals. As there are five free O terminals in this Si—O skeleton, by adding 4H atoms to different terminal O positions, five isomers of the neutral complex clusters can be formed. The optimized structures have energies lying between −3673.8192 and −3673.8430 Hartrees, the lowest energy isomer of which is shown in Figure 6a. These results indicate once again that the Si—O skeleton plays predominant role in determining the energy of the cluster. The positions of the H atoms on terminal O atoms have a minor effect on the energy, which is, however, bigger than the effect of the OH bond directions mentioned before. In Figures 4 and 6, the structural isomers of bare $(SiO_2)_8$ and neutral $(SiO_2)_8O_2H_4$ are arranged in the orders of descending stability, respectively.

Tables 2 and 3 list the energy values of the isomers of the n = 8 bare and complex silica clusters, respectively. Similar to the bare octamer, the complex cluster with an O atom inside the cube cage is more stable than that with the empty cube cage. Here, only the lowest energy cubic complex isomer with energy −3673.8430 Hartrees is included in the table. More interesting is that the cubic complex cluster with an O atom inside the cage is even more stable than the bicage isomer, as will be shown later.

Frequency calculation indicates that the cubic structures of the second magic number clusters $(SiO_2)_8O_2H_4$ with one O atom inside and with the empty cage are both energy minima on the potential energy surfaces. Their zero-point energies are listed in Table 3. Although the empty cube isomer of the bare silica octamer $(SiO_2)_8$ has imaginary frequencies, in the formation of the complex cluster $(SiO_2)_8O_2H_4$ the chemical interaction of the empty cube isomer with 2O and 4H atoms lowers the symmetry of the cluster and thus eliminates the imaginary frequencies, as convinced by our calculation.

The Bicage Isomers of $(SiO_2)_8O_2H_4$

From the neutral first magic number cluster $(SiO_2)_4O_2H_4$, a bicage structure of $(SiO_2)_8O_2H_4$ can be built by doubling the cage structure of $(SiO_2)_4O_2H_4$ through mirror imaging, C_2 axial rotation or center inversion with the elimination of one O_2H_4. The structures formed through different symmetry operations and optimized at the B3LYP/6-31G** level have D_2 and C_{2h} symmetries, respectively, and nearly the same optimized energies. The optimized energy of the D_2 isomer is very slightly lower than that of the C_{2h} isomer. The small energy difference in these structural isomers is due to the difference in the directions of the terminal OH bonds. Frequency calculation of these bicage structures, however, indicates that all these symmetrical isomers have two imaginary frequencies. This means that these bicage structures are not energy minima but are second-order saddle points on the potential energy surface. By distorting the structure to break the symmetry and optimizing again, an isomer with no symmetry is obtained. The energy is lowered to −3673.7762 Hartrees. No imaginary frequencies are found for the distorted bicage structure, indicating that it is an energy minimum. The structure is displayed in Figure 6d and the energy included in Table 3.

A GA search of the $8SiO_2+2O$ configuration space provides several quasi-bicage Si—O skeleton structures with energies next to that of the lowest energy cubic skeleton. Here we shall only show the two quasi-bicage Si—O skeleton structures with lowest energies, denoted as types I and II. Both skeleton structures have five free O terminals, so by adding 4H atoms to different terminal O positions, five isomers of the neutral complex clusters can be formed from each skeleton structure. The optimized structures have energies lying between −3673.8235 and −3673.8375 Hartrees for type I and between −3673.8237 and −3673.8331 Hartrees for type II. On average, these neutral complex clusters have DFT optimized energies slightly higher than that of the lowest energy cubic isomer. For simplicity, only the lowest energy isomers of both types are included in Figure 6 and Table 3. These quasi-bicage isomers have energies much lower than the bicage structure built by doubling the cage structure of the first magic number cluster by symmetry operation shown in the table. The structures shown in the figures clearly indicate that these quisi-bicage isomers are highly distorted. Considering the high intercage interaction in forming these quasi-bicage structures, their lower energies in comparison to the one we built through symmetry operations are reasonable. Frequency calculations show that these lowest energy quasi-bicage isomers have no imaginary frequencies, implying that they are energy minima on the potential energy surface.

For the structures of the bare silica octamer $(SiO_2)_8$, the bicage structure is also considered. It can be formed from the bicage complex cluster $(SiO_2)_8O_2H_4$ by dropping the group of atoms O_2H_4. Two structural isomers can be formed: one is by dropping 1OH and 1H from both ends and the other by dropping 2OH from

Table 4. Optimized Energies of Structural Isomers of Anionic Complex Silica Cluster $[(SiO_2)_8O_2H_3]^-$ Calculated at the B3LYP/6-31+G** Level.

Structure	ZPE (kcal/mol)	E (Hartree)	ZPE + E (Hartree)	Δ(ZPE + E) (Hartree)
Cubic with an O inside	77.59844	−3673.40384	−3673.28019	0
Quasi-bicage (Type I)	77.54494	−3673.39996	−3673.27638	0.00381
Quasi-bicage (Type II)	77.75169	−3673.39864	−3673.27474	0.00545
Bicage	77.96566	−3673.32225	−3673.19802	0.08217
Cubic empty cage	77.11416	−3673.29322	−3673.17033	0.10986
Linear chain	76.15600	−3673.22754	−3673.10618	0.17401

one end and 2H from another end. The former has lower energy and the optimized value is listed in Table 2, and the corresponding structure is shown in Figure 4c. The bare quasi-bicage silica structures are not dealt with here.

The details of the calculation of the cubic and bicage structures of the $n = 8$ clusters are described in Appendices A and B.

The Linear Chain Isomers of $(SiO_2)_8O_2H_4$

The linear chain structures of bare silica octamer and the corresponding complex cluster are also optimized, and their energies included in Tables 2 and 3, respectively. In agreement with the previously reported results, the linear chain isomer of bare silica octamer is the most stable. In contrast, the linear chain isomer of the complex cluster $(SiO_2)_8O_2H_4$ is, however, the least stable of the isomers considered.

Table 2 indicates that the stability order of the bare $n = 8$ silica cluster isomers is linear chain > cube with inside O > bicage > empty cube. The highest stability of the linear chain isomer is in agreement with previous results on small silica clusters.[19–23] Similar to the case of the $n = 4$ cluster, our DFT calculation of the lowest energy isomer found by the genetic algorithm with TTAM potential indicated that this cubic isomer is higher in energy than the linear chain isomer. This disagreement is not out of expectation, because the TTAM potential used in our genetic calculation was developed for the condensed phase siliceous materials, so it is favorable to the formation of 3D structures. The change in stability order from that of the bare cluster shown in Table 2 to the order of the complex cluster shown in Table 3, that is, cube with inside O atom > quasi-bicage > bicage > empty cube > linear chain for the second magic number complex cluster demonstrates the stabilization of the cubic and bicage structures of the complex clusters through the active participation of the group of atoms O_2H_4 in chemical bonding during cluster formation, just as in the case of the first magic number cluster. The much lower energies of the quasi-bicage isomers in comparison with the bicage structure formed through symmetry operation illustrate the stabilization of the quasi-bicage clusters through strong interaction between the two $n = 4$ silica cages.

Using GA in our investigation of magic number silica-containing clusters we have successfully generated a large number of interesting skeleton structures for building the starting magic number cluster structures to be used for subsequent DFT optimization. In particular, the search of the configuration spaces $4SiO_2+2O$ and $8SiO_2+2O$ provides much interesting information about the complex silica clusters, which is difficult to access without the use of such global optimization method. Certainly, other global optimization methods, for example, the basin-hopping algorithm, might also be effective. A discussion on various optimization methods has been presented in Wales' article.[24]

The GA search and the DFT optimization indicate that for the second magic number silica cluster there exists a great variety of possible structural isomers, including both the cubic and bicage series. Although the lowest energy isomer is a cubic one, and the cubic isomers are lower in energy than the quasi-bicage isomers in average, the difference in energy between these two series is quite small, that is, they are nearly iso-energetic. We have also done the DFT optimization of $(SiO_2)_8O_2H_4$ with a larger basis set 6-311G** and found that the stability order remains the same. Therefore, it is more appropriate to assume that the $n = 8$ magic number silica cluster generated in experiments will be a mixture of cubic and quasi-bicage structural isomers, possibly slightly more favorable to the cubic ones. If the bicage structure is the most stable isomer of the second magic number cluster as we thought before, we might expect that there would exist a third magic number cluster at $n = 12$ composed of three $n = 4$ complex cages connected in series. But such magic number cluster has never been observed in our experiments. The higher average stability of the complex cubic structure with inside O atom over the quasi-bicage structures gives theoretical interpretation of our experimental mass spectrometric result, which shows the appearance of only the first and the second magic number clusters at $n = 4$ and $n = 8$. Moreover, even though the second magic cluster might take the quasi-bicage structures, the fact that they are highly distorted through cage interaction and the formation of "tricage" structure would be hardly probable. Hence, from our structure investigation the absence of the third magic number cluster is reasonable.

Up to now we have only discussed the neutral cluster structures. To correlate our calculations with the experiments, we have to look at the anionic case. As discussed in our previous article, proton stripping from neutral complex cluster $(SiO_2)_nO_2H_4$ would give $[(SiO_2)_nO_2H_3]^-$, which just matches the experimentally observed composition of the magic number cluster sequence. From each of the cubic and the quasi-bicage $(SiO_2)_8O_2H_4$ clusters, derived from GA calculation, 10 anionic isomers can be formed by stripping proton from nonequivalent H sites of the neutral cluster. In the less stable neutral cubic empty cage cluster, there are two nonequivalent H sites, so two anionic isomers can be formed. The energies of the bicage and linear chain anionic complex clusters

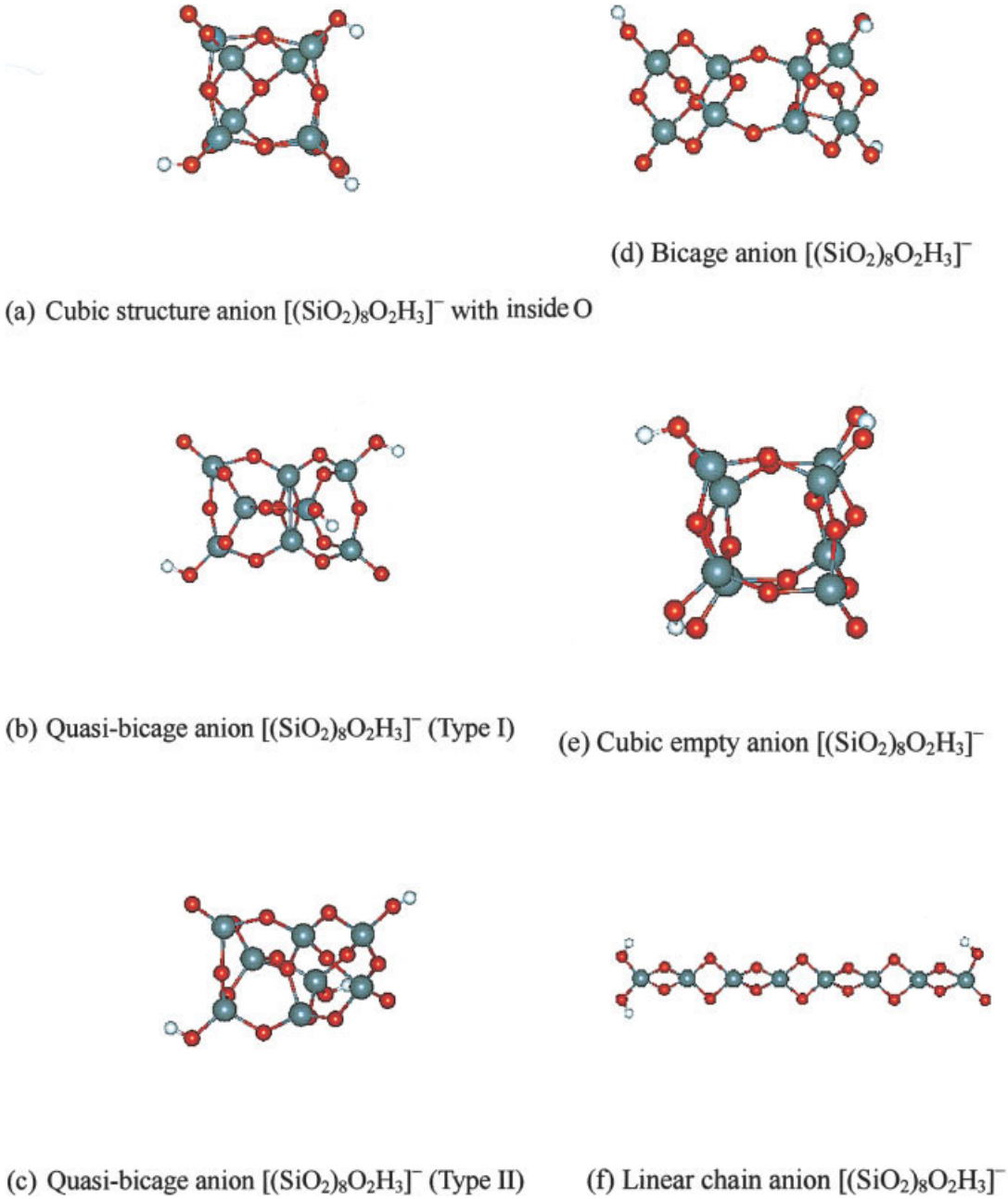

Figure 7. B3LYP/6-31+G** optimized structures of the ground state and the next higher energy isomers of the anionic $[(SiO_2)_8O_2H_3]^-$ complex clusters in the order of descending stability: (a) cubic structure with an O inside the cage, (b) quasi-bicage structure (Type I), (c) quasi-bicage structure (Type II), (d) bicage structure, (e) cubic empty structure, and (f) linear chain structure. [Color figure can be viewed in the online issue, which is available at www.interscience.wiley.com.]

are also optimized. The lowest energy anionic isomers corresponding to the six types of neutral complex clusters are included in Table 4 and the corresponding structures are shown in Figure 7. All the anionic clusters are optimized at the B3LYP/6-31+G** level.

A comparison of Figures 6 and 7 shows that proton stripping does not change the structures much and the stability order remains unchanged as shown in the tables. But for the anionic magic number cluster the quasi-bicage isomers of these two different structural types have practically the same lowest energy, which is very near to that of the cubic one. Frequency calculations confirm that all the anionic complex isomers listed in the table are energy minima on the potential energy surface.

The difference between the energy values listed in the Tables 3 and 4 gives the adiabatic energy of proton stripping. Calculations indicate that the lowest energy isomers of the cubic and quasi-bicage structures have practically the same adiabatic energy of proton stripping. It is 11.5–11.6 eV. The adiabatic energy of proton stripping of the bicage isomer is somewhat higher. It is 12.0 eV. Therefore the energy of proton stripping also supports our supposition that the second magic number cluster is most probably a mixture of cubic and quasi-bicage structural isomers.

Conclusion

Magic number silica clusters $[(SiO_2)_nO_2H_3]^-$ with $n = 4$ and 8 have been generated by XeCl excimer laser (308 nm) ablation of a variety of porous siliceous materials. DFT study indicates that the first anionic magic number cluster $[(SiO_2)_4O_2H_3]^-$ will most probably take the pseudotetrahedral cage structure. Our detailed calculation of the structural isomers of the second magic number silica cluster shows that there exists a great variety of cubic and bicage isomers, including quasi-cubic and quasi-bicage isomers. Here, the merits of genetic algorithm in the investigation of cluster structures are obvious. The lowest energy cubic and quasi-bicage isomers (neutral and anionic) have only small energy differences. From the energy values we obtained up to now, we can say that the ground-state isomer may have the cubic cage-like structure with an O atom inside the cage, which has energy slightly lower than those of the quasi-bicage isomers. But because there are many cubic and quasi-bicage isomers having similar energies, we think that the experimentally generated second magic number cluster might be a mixture of various cubic and quasi-bicage isomers, possibly slightly more favorable to the cubic ones. The slightly higher stability of the cubic cage structure over the quasi-bicage structures and the serious distortion of the quasi-bicage isomers might give a reasonable interpretation of the absence of the third magic number cluster in our mass spectra. Theoretical calculation demonstrates the stabilization of the complex magic number clusters through the active participation of the group of atoms 2O and 4H (3H for the anion) in chemical bonding during cluster formation.

Acknowledgments

We are grateful to Prof. Jue Wang and his colleagues at Tongji University, Prof. Yingcai Long at the Chemistry Department of Fudan University and Prof. Liying Liu at the Department of Optical Science and Engineering for providing the silica samples.

References

1. Zhao, L.; Zhu, L.; Liu, L.; Zhang, J.; Li, Y. F.; Zhang, B.; Shen, J.; Wang, J. Chem Phys Lett 1996, 255, 142.
2. Xu, C.; Wang, L.; Qian, S. X.; Zhao, L.; Wang, Z.; Li, Y. F. Chem Phys Lett 1997, 281, 426.
3. Xu, C.; Long, Y. C.; Zhang, R.; Zhao, L.; Qian, S. X.; Li, Y. F. Appl Phys A 1998, 66, 99.
4. Wang, C.; Liu, L.; Li, Y. F. Acta Phys Chim Sin 1999, 15, 139 (in Chinese).
5. Xu, C.; Wang, W. N.; Zhang, W.; Zhuang, J.; Liu, L.; Kong, Q. Y.; Zhao, L.; Long, Y. C.; Fan, K. N.; Qian, S. X.; Li, Y. F. J Phys Chem A 2000, 104, 9518.
6. Frisch, M. J.; Trucks, G. W.; Schlegel, H. B.; Scuseria, G. E.; Robb, M. A.; Cheeseman, J. R.; Zakrzewski, V. G.; Montgomery, J. A., Jr.; Stratmann, R. E.; Burant, J. C.; Dapprich, S.; Millam, J. M.; Daniels, A. D.; Kudin, K. N.; Strain, M. C.; Farkas, O.; Tomasi, J.; Barone, V.; Cossi, M.; Cammi, R.; Mennucci, B.; Pomelli, C.; Adamo, C.; Clifford, S.; Ochterski, J.; Petersson, G. A.; Ayala, P. Y.; Cui, Q.; Morokuma, K.; Malick, D. K.; Rabuck, A. D.; Raghavachari, K.; Foresman, J. B.; Cioslowski, J.; Ortiz, J. V.; Baboul, A. G.; Stefanov, B. B.; Liu, G.; Liashenko, A.; Piskorz, P.; Komaromi, I.; Gomperts, R.; Martin, R. L.; Fox, D. J.; Keith, T.; Al-Laham, M. A.; Peng, C. Y.; Nanayakkara, A.; Gonzalez, C.; Challacombe, M.; Gill, P. M. W.; Johnson, B.; Chen, W.; Wong, M. W.; Andres, J. L.; Gonzalez, C.; Head–Gordon, M.; Replogle, E. S.; Pople, J. A. Gaussian 98, Revision A.7; Gaussian, Inc.: Pittsburgh, PA, 1998.
7. Becke, A. D. J Chem Phys 1993, 98, 5648.
8. Lee, C.; Yang, E.; Parr, R. G. Phys Rev B 1988, 37, 785.
9. Bauschlicher, C. W.; Ricca, A.; Partridge, H.; Langhoff, S. R. In Recent Advances in Density Functional Theory; Chong, D. P., Ed.; World Scientific Publishing: Singapore, 1997, Part II.
10. Siegbahn, P. E. M. Adv Chem Phys 1996, XCIII.
11. Bytheway, I.; Wong, M. W. Chem Phys Lett 1998, 282, 219.
12. Petersson, G. A.; Al-Laham, M. A. J Chem Phys 1991, 94, 6081.
13. Petersson, G. A.; Bennett, A.; Tensfeldt, T. G.; Al-Laham, M. A.; Shirley, W. A.; Mantzaris, J. J Chem Phys 1988, 89, 2193.
14. Deaven, D. M.; Ho, K. M. Phys Rev Lett 1995, 75, 288.
15. Zhang, W.; Liu, L.; Zhuang, J.; Li, Y. F. Phys Rev B 2000, 62, 8276.
16. Zhuang, J.; Kojima, T.; Zhang, W.; Liu, L.; Zhao, L.; Li, Y. F. Phys Rev B 2002, 65, 45411.
17. Zhuang, J.; Sun, Z. H.; Zhang, W.; Zhuang, M.; Ning, X. J.; Liu, L.; Li, Y. F. Phys Rev B 2004, 69, 165421.
18. Harkless, J. A. W.; Stillinger, D. K.; Stillinger, F. H. J Phys Chem 1996, 100, 1098.
19. Wang, L. S.; Wu, H.; Desai, S. R.; Fan, J.; Colson, S. D. J Phys Chem 1996, 100, 8697.
20. Fan, J.; Nicholas, J. B.; Price, J. M.; Colson, S. D.; Wang, L. S. J Am Chem Soc 1995, 117, 5417.
21. Wang, L. S.; Nicholas, J. B.; Dupuis, M.; Wu, H.; Colson, S. D. Phys Rev Let. 1997, 78, 4450.
22. Wang, L. S.; Desai, S. R.; Wu, H.; Nicholas, J. B. Z. Phys D 1997, 40, 36.
23. Nayak, S. K.; Rao, B. K.; Khanna, S. N.; Jena, P. J Chem Phys 1998, 109, 1245.
24. Wales, D. J.; Doye, J. P. K. J Phys Chem A 1997, 101, 511.

Appendix A

Calculation of $n = 8$ Cubic Silica Clusters

Cubic Octamer with Empty Cage

Optimization of the simple cubic structure of $(SiO_2)_8$ composed of eight Si—O tetrahedrons gives the D_2 structure (a). Frequency calculation shows imaginary frequencies. By distorting the mole-

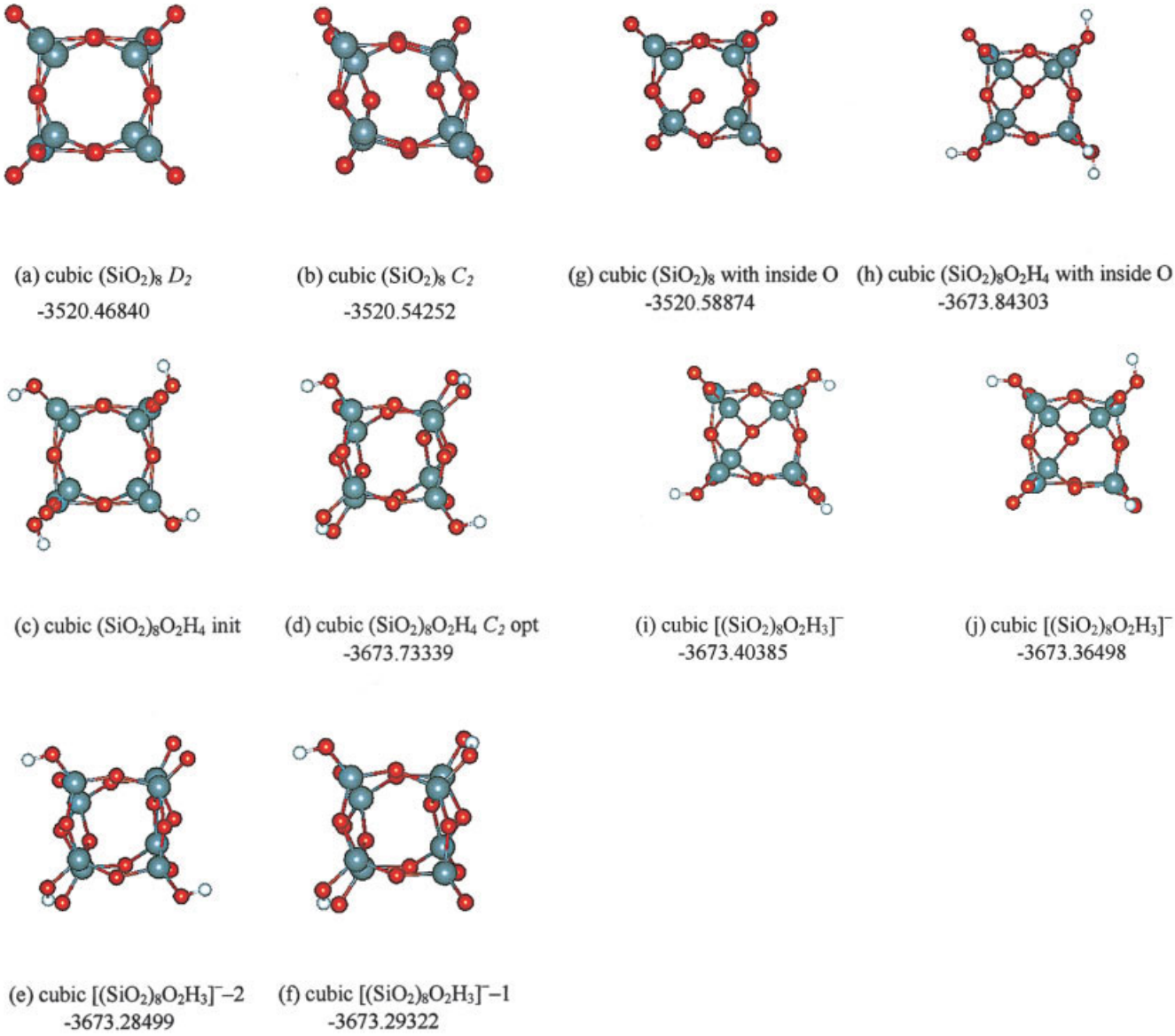

Appendix A. [Color figure can be viewed in the online issue, which is available at www.interscience.wiley.com.]

cule and reoptimizing, structure (b) is obtained, which is lower in energy than structure (a) and has no imaginary frequency.

Addition of the group of atoms O_2H_4 to the proper sites of structure (a) gives the starting configuration (c) of $(SiO_2)_8O_2H_4$ for optimization. Chemical interaction of the group of atoms O_2H_4 with the cubic $(SiO_2)_8$ cage causes the distortion of the cubic skeleton on optimization to form structure (d) of $(SiO_2)_8O_2H_4$ with C_2 symmetry, which has no imaginary frequency. Addition of O_2H_4 to structure (b) gives the same structure (d). This structure of $(SiO_2)_8O_2H_4$ is included in Figure 6 and Table 3, and only structure (a) of $(SiO_2)_8$ is included in Figure 4 and Table 2.

In structure (d) there are two nonequivalent H sites. Therefore, proton stripping will give two isomers of anionic complex cluster $[(SiO_2)_8O_2H_3]^-$ shown in (e) and (f), the DFT energies of which are −3673.28499 and −3673.29322 Hartrees, respectively. The lower energy isomer is included in Figure 7 and Table 4.

Cubic Octamer with an O Atom Inside the Cage

Genetic algorithm search of the $8SiO_2$ configuration space gives the lowest energy isomer of the silica octamer $(SiO_2)_8$, which has an O atom inside the cubic cage. DFT calculation indicates that this isomer, as shown in Figure (g), is more stable than the empty cage isomer (b), vibrational analysis shows no imaginary frequency for this isomer.

GA search of $8SiO_2+2O$ space gives the lowest energy skeleton, which is also a structure with an O atom inside the

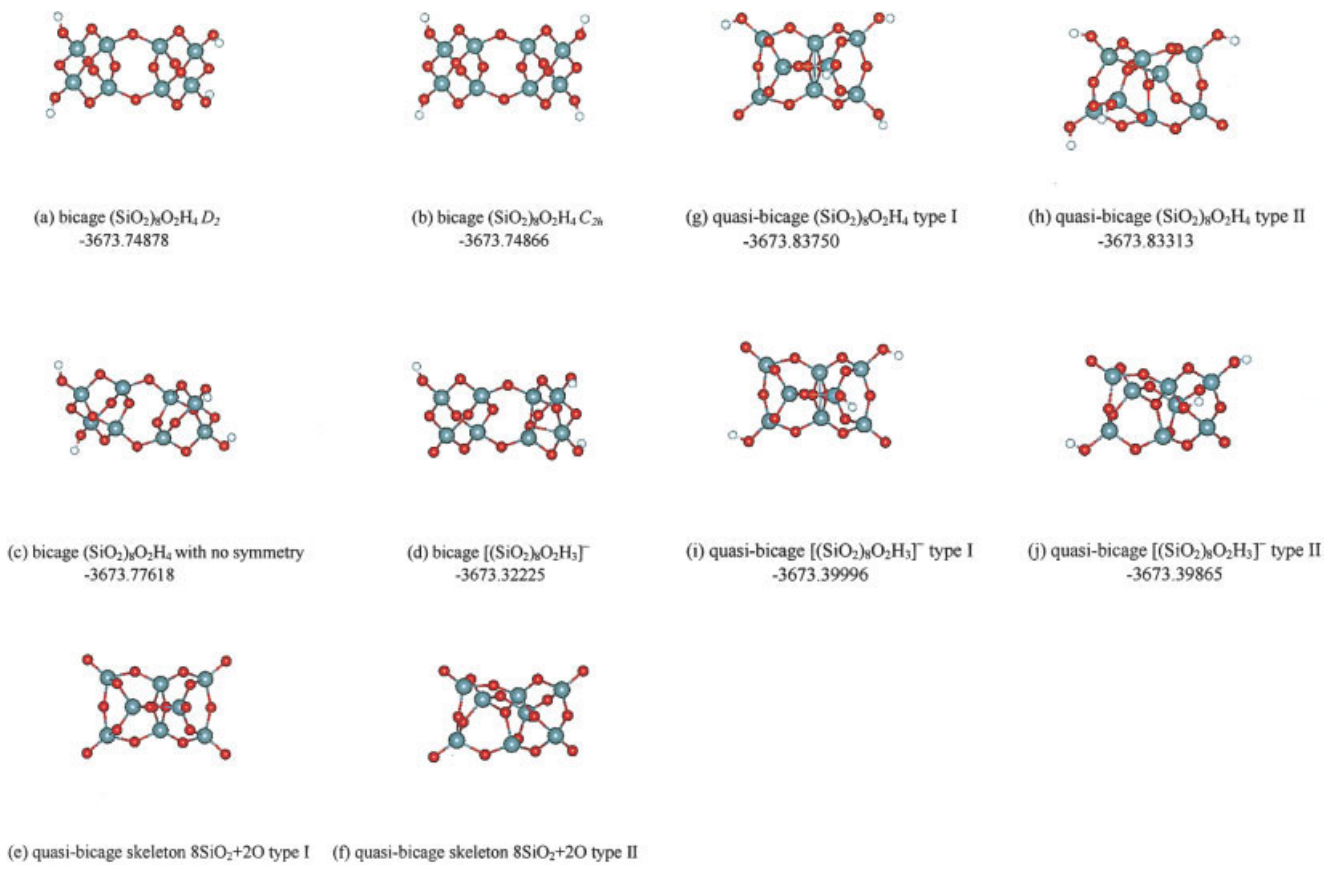

Appendix B. [Color figure can be viewed in the online issue, which is available at www.interscience.wiley.com.]

cubic cage but has two additional terminal O atoms. The skeleton structure has five free terminal O atoms, so addition of H atoms to four of the free terminal O atoms can form five isomers of the neutral complex cluster $(SiO_2)_8O_2H_4$. The energies of these isomers after DFT optimization lie between −3673.8192 and −3673.8430 Hartrees, the lowest energy structure is shown in (h). Similar to the case of bare $(SiO_2)_8$ isomers, the complex isomer with an O atom inside the cage is more stable than the empty cage complex isomer.

The magic number cluster appearing in the mass spectra is the anionic complex cluster $[(SiO_2)_8O_2H_3]^-$, which can be formed from proton stripping of the neutral complex cluster $(SiO_2)_8O_2H_4$. In each of the neutral complex isomer such as structure (h), there are four nonequivalent H sites. Therefore, proton stripping will give four isomers of anionic complex cluster $[(SiO_2)_8O_2H_3]^-$. We can also regard the anionic complex cluster as formed by adding H atoms to three of the terminal O atoms of the $8SiO_2$+2O skeleton structure. As there are five nonequivalent H sites in the skeleton, altogether 10 anionic isomers can be formed. We have calculated the DFT energies of all the possible anionic isomers formed from the cubic $8SiO_2$+2O skeleton, which lie between −3673.3650 and −3673.4038 Hartrees, the lowest and the highest energy structures are shown in (i) and (j), respectively. The structures shown indicates that the anionic isomers have the same skeleton and the difference in energies originates from the different sites of the H atoms. Note that the OH bond directions will also affect the energy of the molecule, but the effect is usually small and so in our article this effect is neglected unless it causes the appearance of imaginary frequencies.

Appendix B

Calculation of n = *8 Bicage Silica Clusters*

Bicage Octamer Built through Symmetry Operation

Another probable structure of the second magic number silica cluster is of the bicage type. From the neutral first magic number cluster $(SiO_2)_4O_2H_4$, a bicage structure of $(SiO_2)_8O_2H_4$ can be built by doubling the cage structure of $(SiO_2)_4O_2H_4$ through mirror imaging, C_2 axial rotation or center inversion with the elimination of one O_2H_4. The structures formed through different symmetry operations and optimized at the B3LYP/6-31G** level have D_2 or C_{2h} symmetry and nearly the same optimized energies as shown in figures (a) and (b), respectively. Symmetry constraint imposed by the symmetry operation in doubling the cage structure leads to

imaginary frequencies of the resulting bicage structures. By unconstraining the symmetry in performing the structure optimization, the distorted structure (c) with no symmetry is obtained. The elimination of the imaginary frequencies demonstrates that an energy minimum is reached. This is the bicage isomer listed in Table 3. Anionic complex cluster $[(SiO_2)_8O_2H_3]^-$ can be formed by proton stripping of either structure (a) or structure (b). Optimization gives the distorted structure (d). It is easy to predict that such structure is an energy minimum without imaginary frequency, as confirmed by our calculation. The optimized energy is −3673.32225 Hartrees. Anionic complex cluster $[(SiO_2)_8O_2H_3]^-$ can also be formed from structure (c), the optimized energy of which is −3673.31857 Hartrees, slightly higher than that of (d). So the energy value of (d) is included in Table 4.

The structure of the bicage bare octamer $(SiO_2)_8$ has already been described and will not be repeated here.

Quasi-bicage Octamer from GA Search

GA search of $8SiO_2+2O$ space gives several quasi-bicage skeleton structures with energies higher than that of the lowest energy cubic skeleton. Two of the skeleton structures next in energy to the cubic one are shown in Figures (e) and (f), and called types I and II, respectively. The type II structure is highly distorted. Similar to the cubic skeleton discussed above, in each skeleton structure there are five free terminal O atoms, so addition of H atoms to four of the free terminal O atoms can form five isomers of the neutral complex cluster $(SiO_2)_8O_2H_4$ and addition of H atoms to three of the free terminal O atoms can form 10 isomers of the anionic complex cluster $[(SiO_2)_8O_2H_3]^-$. The energies of the neutral quasi-bicage isomers after DFT optimization lie between −3673.8235 and −3673.8375 Hartrees for type I and between −3673.8237 and −3673.8331 Hartrees for type II skeletons, respectively. The lowest energy structures are shown in Figures (g) and (h). The energies of the anionic quasi-bicage isomers lie between −3673.3639 and −3673.4000 Hartrees for type I and between −3673.3690 and −3673.3986 Hartrees for type II skeletons, respectively. The lowest energy anionic quasi-bicage structures are shown in Figures (i) and (j). By comparison, we find that the type I and type II quasi-bicage structures are quite different, but their energies, both the neutral and the anionic clusters, are very similar. These energies are also near to the energies of the cubic isomers. Nevertheless, the lowest energy isomer of the magic number silica cluster with $n = 8$, both the neutral and the anionic, has the cubic structure.